Journal of the Korean Ceramic Society (2024) 61:654–660
https://doi.org/10.1007/s43207-024-00392-y

ORIGINAL ARTICLE

Understanding thermal depolarization via thermally stimulated depolarization current measurement

Jeong-Woo Sun[1,2] · Temesgen Tadeyos Zate[1] · Woo-Jin Choi[1] · Geon-Ju Lee[1] · Sang-Goo Lee[3] · Jong Eun Ryu[2] · Wook Jo[1]

Received: 8 November 2023 / Revised: 27 February 2024 / Accepted: 14 March 2024 / Published online: 15 April 2024

Abstract
Thermal depolarization in poling-induced piezoelectric materials is defined as the disappearance of remanent polarization at a so-called depolarization temperature. A thermally stimulated depolarization current (TSDC) measurement is most widely used for examining depolarization as a function of temperature. TSDC results in the literature commonly show a gradual reduction of polarization even below depolarization temperature (T_d). However, no degradation happens when thermal heat treatments are conducted below T_d, meaning that the apparent reduction in polarization measured by TSDC is sure to be an artifact. Here, we demonstrate that such artifact is unavoidable during TSDC measurements and propose a method to circumvent it. This strategy was manifested on TSDC data collected from a relaxor ferroelectric $Pb(Mg_{1/3}Nb_{2/3})O_3$-$PbTiO_3$ (PMN-PT) single crystals.

Keywords Thermally stimulated depolarization current · Depolarization temperature · PMN-PT · Single crystal · Phase transformation

1 Introduction

Piezoelectric materials, which accumulate the electric charge with respect to applied stress or vice versa, have been attributed to a range of applications such as actuators, ultrasonics, transducers, and so on [1–3]. Starting from polycrystalline $BaTiO_3$, ferroelectric-based piezoelectric ceramics have been developed through morphotropic phase boundary (MPB) composition [4–7], composite-like structure [8–10], textured ceramics [11, 12], and defect chemistry by doping with a donor or an acceptor [13–15]. Recently, relaxor ferroelectric single crystals such as $Pb(Mg_{1/3}Nb_{2/3})O_3$-$PbTiO_3$ (PMN-PT) and $Pb(Zn_{1/3}Nb_{2/3})O_3$-$PbTiO_3$ (PZN-PT) have been attracted due to its high piezoelectric coefficient ($d_{33} > 1500$ pC/N) and electromechanical coupling factor ($k_{33} > 0.90$) [16–19]. For applications to the piezoelectricity, the above materials require electrical poling which is a post-treatment to change the domain configuration from a randomly oriented state to aligned polarization vectors along a specific direction by applying an external electric field [20, 21]. It is commonly accepted that the ferroelectric materials lose their aligned polarization state at Curie temperature (T_C), which is a ferroelectric-to-paraelectric phase transformation temperature [22, 23]. In fact, thermal depolarization in the poled ferroelectric materials occurs at an elevated temperature but below T_C, the so-called depolarization temperature (T_d), due to thermal activation such as a structural change and a defect migration [24–26]. On the other hand, relaxor ferroelectrics, which exhibit a strong frequency dependence, have been considered to be the origin of thermal depolarization by a ferroelectric-to-relaxor phase transformation below dielectric maximum temperature (T_m) [27–29]. From the viewpoint of thermal stability, the operating temperature of poled piezoelectric materials can stand a chance to be lower than T_C or T_m because the degradation of piezoelectricity can be designated in the vicinity of T_d [30–33]. In this regard, understanding T_d has importance to determine the operating temperature of piezoelectric

✉ Wook Jo
wookjo@unist.ac.kr

[1] Department of Materials Science and Engineering, Ulsan National Institute of Science and Technology, Ulsan 44919, Republic of Korea

[2] Department of Mechanical and Aerospace Engineering, North Carolina State University, Raleigh, NC 27695, USA

[3] iBULe Photonics, Inc., 7-39, Songdo-dong, Yeonsu-gu, Incheon 21999, Republic of Korea

materials free from thermal fluctuation or degradation of the properties.

For the investigation of thermal depolarization, a thermally stimulated depolarization current (TSDC) has been measured in response to a change in the dipole moment from the materials as a function of temperature [34]. In addition, the TSDC measurement is advantageous to compute the remanent polarization (P_r) by integrating the currents with respect to time to calculate the amount of electric charge [35]. Even though the P_r tends to decrease with elevating temperature owing to the thermal activation of aligned domains, previous TSDC results show the reduction of polarization even below T_d of the poled materials [36–39]. Moreover, the different temperature-dependent reductions of P_r observed in the literature make it challenging to conduct an accurate and detailed quantitative analysis of P_r in regard to temperature. Since the TSDC measurement collects nanoscopic signals arising from the loaded sample, undesired background currents can be measured below T_d. Therefore, these currents are essential to differentiate between genuine signals and any artifacts that might be present. The distinction between them holds significance for analyzing the changes of the properties due to thermal depolarization and determining the operating temperature of piezoelectric materials.

Here, we investigate the thermal depolarization of a relaxor ferroelectric PMN-PT single crystals. Our approach encompasses temperature-dependent dielectric measurements and in situ X-ray diffraction (XRD) to discover a correlation between T_d and crystalline phase transformations. We employ thermal heat treatments in these materials for comparing the electrical properties after heat treatment below and above T_d through impedance and polarization analyses. From TSDC data, we identify the small currents detected below T_d to determine their nature whether a measurement artifact or a genuine depolarization signal. Since no degradation occurs when heat treatments are performed below T_d, the apparent decrease in polarization measured by TSDC is clear to be an artifact. We demonstrate that such artifact is inevitable during TSDC measurements and propose a method to circumvent it. The results of this study will contribute to understanding thermal depolarization and quantitative TSDC analyses of piezoelectrics.

2 Experimental

[001]-oriented rhombohedral PMN-PT single crystals were prepared by the vertical Bridgman method at iBULe Photonics Co. Ltd. (Incheon, Republic of Korea). PMN-PT single crystals were cut into the $4 \times 4 \times 0.5$ mm from the grown crystal boule along the growth direction with gold electrodes which were vacuum-sputtered on the (001) plane to measure the electrical properties. For the engineering of the ferroelectric domains, conventional direct current (DC) poling was applied on the samples by an external electric field at 1 kV/mm and 25 ℃ for 1 min using a commercial apparatus, aixPES (aixACCT Systems GmbH, Aachen, Germany).

To investigate the phase transformations, the dielectric properties were measured using a Novocontrol broadband dielectric spectrometer (Novocontrol Technologies GmbH & Co. KG, Hundsangen, Germany) equipped with a temperature controller over the temperature range from 25 to 200 ℃ at the heating rate of 3 ℃/min. The measurement frequencies were 10 Hz, 100 Hz, 1 kHz, and 10 kHz to record the frequency dependence at constant temperatures. The temperature-dependent crystalline phases were characterized by in situ X-ray diffraction (XRD) (SmartLab, Rigaku Co., Tokyo, Japan) equipped with a high-temperature attachment using an incident beam of Cu-$K\alpha$ ($\lambda = 1.5406$ Å) radiation. The XRD patterns were obtained in a step size of 0.01° for a 2θ scanning range of 40–50° to investigate the (200) reflection of the samples. To characterize thermal depolarization, a heat treatment, *i.e.*, heating up to a set temperature and subsequently cooling back to 25 ℃, was performed for a comparison of the heat treatment below and above T_d and evaluated the thermally activated electrical properties. The longitudinal piezoelectric coefficient (d_{33}) was measured at least 5 times using a commercial Berlincourt-type d_{33} meter (YE2730A, SINOCERA, Yangzhou, China). The impedance analyses of the thickness vibration modes were carried out to inspect the piezoelectric resonance and anti-resonance using a multi-frequency LCR meter (HP 4194A, Agilent Technologies, Santa Clara, USA) with an Agilent 16034E test fixture. Capacitance and dielectric loss ($\tan \delta$) were measured using the LCR meter and relative dielectric permittivity (ε_r) was calculated from the recorded capacitance. The electric field-dependent polarization and current curves were analyzed to investigate the poled state at a condition of ± 1 kV/mm, 1 Hz, and 25 ℃ using the aixPES systems.

From thermally stimulated depolarization current (TSDC) measurement, the depolarization of PMN-PT single crystals was monitored as a function of temperature using a Model 486 picoammeter (Keithley Instruments Inc., Cleveland, Ohio, USA) at the heating/cooling rate of 3 ℃/min. The measurements of depolarization current were taken at 0.5 s intervals. Remanent polarization (P_r) was calculated by integrating currents in respect of time to determine the electric charge, *i.e.*, $Q = \int i(t)dt$, and dividing an area of the samples on the assumption to be equivalent to a surface charge density in the case of a high relative permittivity [40]. In this paper, two results of temperature-dependent P_r (*i.e.*, Calculated P_r and Corrected P_r) were derived from

the currents; before background correction using original data and after background correction with subtraction of a baseline to circumvent the measurement artifacts. For background correction, we generated the baseline corresponding to the artifacts based on the experimental results and fitted the depolarization current to ensure the reliability of the TSDC measurements.

3 Results and discussion

The phase transformation of ferroelectric materials is accompanied by a peak of tan δ due to the structural softening upon the macroscopic response [21, 23]. In Fig. 1a, dielectric permittivity (ε_r) and dielectric loss (tan δ) of the PMN-PT single crystals were measured with increasing temperature to determine the phase transformation temperatures. It is generally accepted that [001]-poled rhombohedral PMN-PT single crystals undergo twofold phase transformations from a rhombohedral to a tetragonal structure at $T_{R\text{-}T}$ and from the tetragonal to a cubic structure at T_C [41–43]. As shown in tan δ curves, the peaks were shown at two temperatures of the steepest increase, *i.e.*, $T_{R\text{-}T}$ (~98 ℃) and T_C (~130 ℃), considering these materials can be faced with thermally induced phase transformations. From the frequency dependence, two tan δ peaks appeared at each phase transformation temperature regardless of the frequency, implying that such dielectric anomalies revealed a series of ferroelectric phase transformations with long-range order. On the other hand, Fig. 1b showed in situ XRD patterns to investigate the structural properties with elevating temperature. A tetragonal splitting of the (200) reflection visible by the narrower intensity on the low 2θ part of the diffraction peak rapidly appeared in the temperature range of 95–100 ˚C. The emergence of the tetragonal splitting can take place a structural change from the rhombohedral to the tetragonal crystalline phases, which provided a good agreement with the first tan δ peak from Fig. 1a. Notably, $T_{R\text{-}T}$ of [001]-poled rhombohedral PMN-PT single crystals has been identified as depolarization temperature (T_d) where aligned ferroelectric domains revert back to a randomly oriented polarization state. In that sense, T_d of these materials was considered to be ~98 ℃, and the thermal depolarization was discussed on the basis of T_d.

The heat treatment, *i.e.*, heating up to a set temperature and subsequently cooling back to 25 ˚C, was performed to investigate the thermally induced depolarization as shown in Fig. 2. The reduced temperature (T/T_d) is defined as a heating temperature (T) divided by T_d. The T/T_d is lower than 1 when the heating temperature is lower than T_d, and the T/T_d is higher than 1 when the heating temperature is higher than T_d. It is important to note that the electrical properties including piezoelectric coefficient

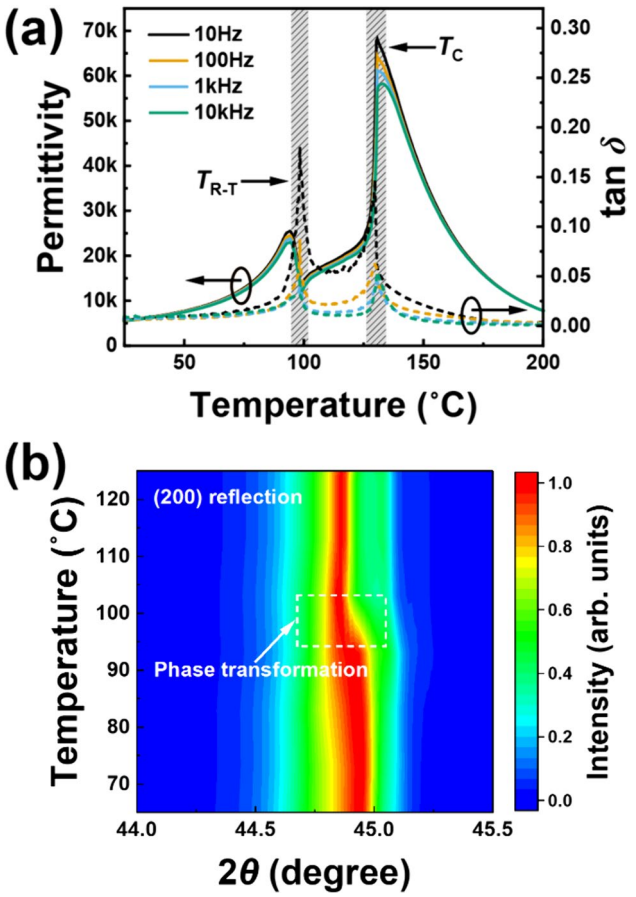

Fig. 1 **a** Temperature dependence of relative dielectric permittivity (ε_r, solid line) and dielectric loss (tan δ, dashed line) of [001]-poled rhombohedral PMN-PT single crystals at 10 Hz, 100 Hz, 1 kHz, and 10 kHz [$T_{R\text{-}T}$ = ~98 ℃, T_C = ~130 ℃] and **b** in situ X-ray diffraction (XRD) analyses of the (200) reflection for temperatures ranging from 70 to 120 ℃

(d_{33} ~ 1480 pC/N at 25 ℃), electromechanical coupling factor (k_t ~ 0.54 at 25 ℃), relative dielectric permittivity (ε_r ~ 5300 at 25 ℃), and dielectric loss (tan δ ~ 0.0063 at 25 ℃) preserved after heat treatment below T_d. Given that the electric properties signify the ability to hold an electrical charge and of charge accumulation from a mechanical stress, the piezoelectricity of [001]-poled PMN-PT single crystals was surely sustained after heat treatment below T_d. However, the piezoelectric and dielectric properties were degraded after heat treatment above T_d because of thermal depolarization. The depolarization of these materials may be attributed to rhombohedral-to-tetragonal phase transformation in the vicinity of T_d. In conclusion, the electrical properties of [001]-poled rhombohedral PMN-PT single crystals persisted up to T_d, and the deterioration of piezoelectric and dielectric activities was detected after heat treatment above T_d.

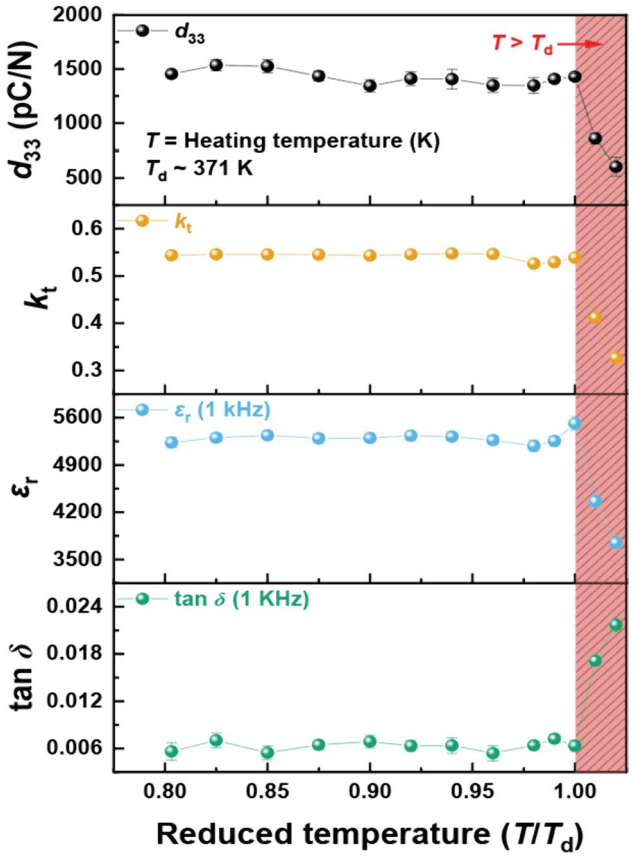

Fig. 2 Electrical properties of [001]-poled rhombohedral PMN-PT single crystals after heat treatment including piezoelectric coefficient (d_{33}), electromechanical coupling factor (k_t), relative dielectric permittivity (ε_r) at 1 kHz, and dielectric loss (tan δ) at 1 kHz

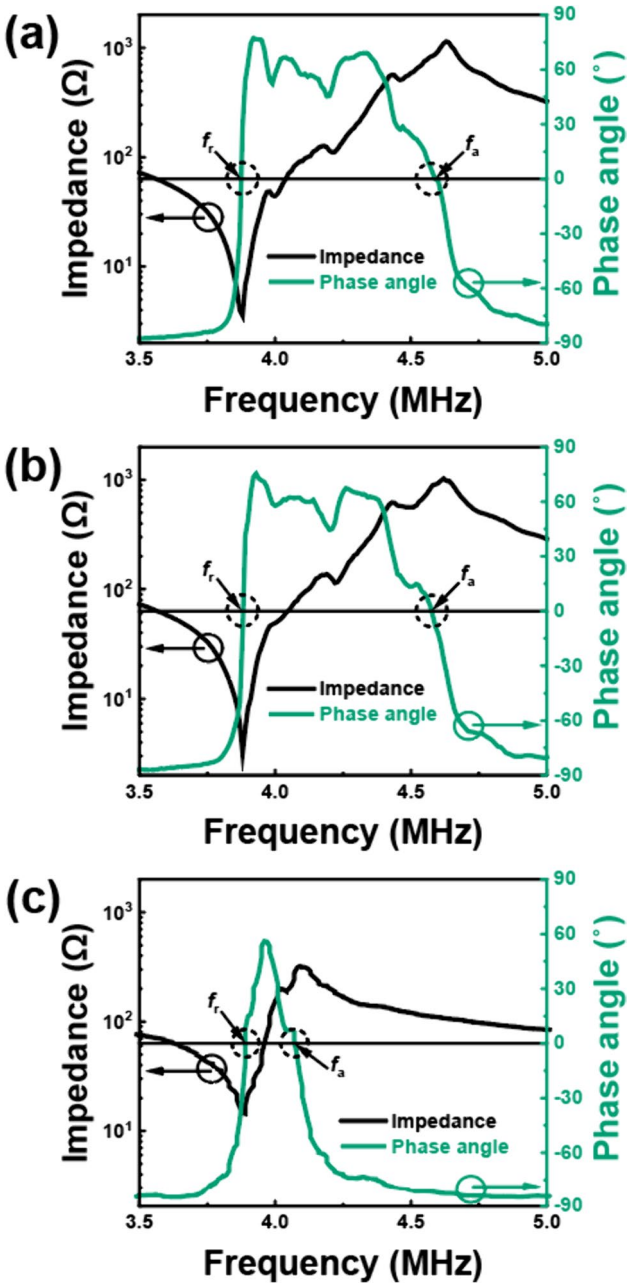

Fig. 3 Impedance and phase angle spectra for [001]-poled rhombohedral PMN-PT single crystals of the thickness vibration modes; **a** before heat treatment, **b** after heat treatment below T_d, and **c** after heat treatment above T_d

In Fig. 3, electromechanical impedance analyses were performed using [001]-poled PMN-PT single crystals to characterize how the poled state of the samples was changed according to the heat treatment. The samples were measured by the thickness vibration modes to investigate the resonance and anti-resonance modes at the frequency range from 3.5 to 5.0 MHz. It is notable that the identical frequencies of resonance (f_r ~ 3.88 MHz) and anti-resonance (f_a ~ 4.63 MHz) mode were detected in Fig. 3a and b, implying that both have an equivalent electromechanical coupling factor (k_t ~ 0.54) which is certainly relevant to the degree of poling. Furthermore, the phase angle was each similar as shown in Fig. 3a and b where the highest theta values were found to be 77.3° and 77.1°, respectively, though some satellite peaks were observed on the spectra for the thickness vibration mode. On the other hand, Fig. 3c showed the obvious depolarization of piezoelectric single crystals owing to the degradation of the electromechanical coupling factor (k_t ~ 0.32). In addition, f_r was equivalent after heat treatment above T_d which indicated the identical elastic compliance, density, and dimension of the specimens regardless of the depolarization. However, f_a was notably decreased since the depolarization probably decreased the longitudinal piezoelectric coefficient (d_{33}) and dielectric permittivity (ε_{33}). To conclude, the electromechanical properties for [001]-poled rhombohedral PMN-PT single crystals were maintained after heat treatment below T_d, whereas they were degraded after heat treatment above T_d due to thermal depolarization.

Polarization and switching current were measured by an external electric field to investigate how the heat treatment affects the ferroelectric properties of [001]-poled PMN-PT single crystals as shown in Fig. 4. It is noticeable that Fig. 4a and b indicated no current peak in the positive range of the electric field. In addition, they exhibited similar remanent polarization (P_r) in which the P_r of Fig. 4a and b showed 23.9 μC/cm^2 and 23.8 μC/cm^2, respectively, implying there was no depolarization after heat treatment

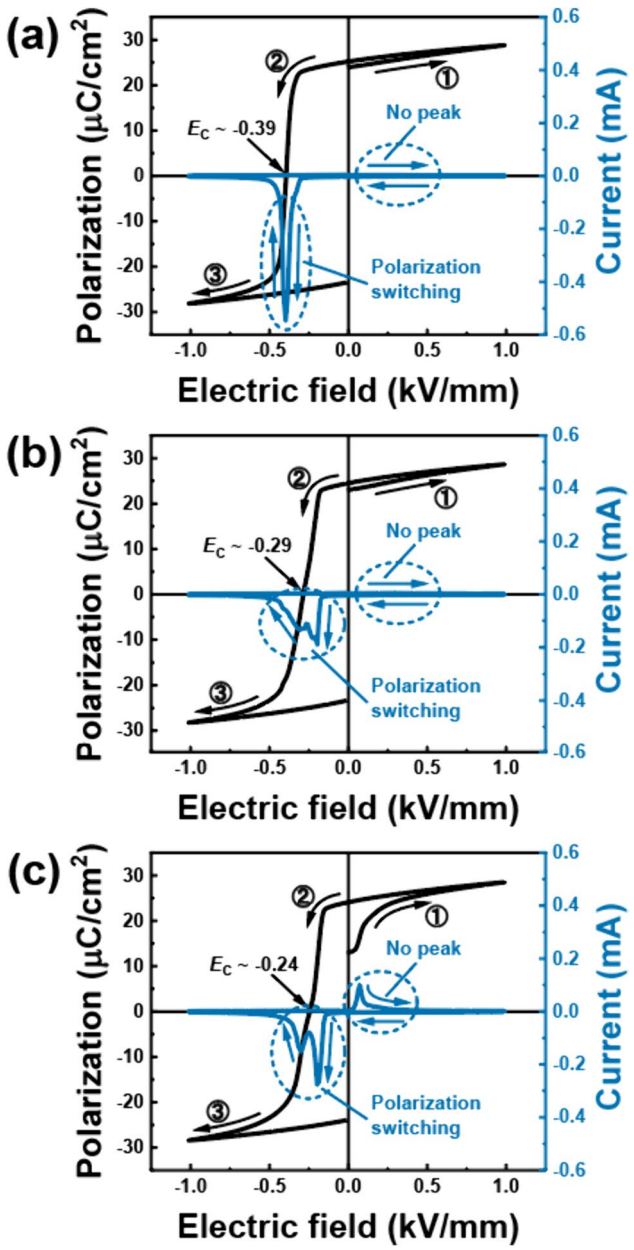

Fig. 4 Polarization *vs.* electric field (P-E) and current *vs.* electric field (I-E) curves for [001]-poled rhombohedral PMN-PT single crystals without pre-polarization; **a** before heat treatment, **b** after heat treatment below T_d, and **c** after heat treatment above T_d

below T_d. During the reverse cycle of the electric field, the electric field-dependent current peak at a negative coercive field (E_C) indicates the ferroelectric domain switching along the reverse direction. It is notable that a polarization reversal occurred at E_C in both Fig. 4a (E_C ~ -0.39 kV/mm) and Fig. 4b (E_C ~ -0.29 kV/mm). Given the observed changes in negative E_C and current peak intensity, thermal activation might induce variations in the ferroelectric domain configuration. Nonetheless, it was clarified that the depolarization was not detected after heat treatment below T_d, considering similar P_r and no current peak in the range of positive electric field. It is expected that the macroscopic long-range order of [001]-poled rhombohedral PMN-PT single crystals would not collapse below T_d. On the other hand, Fig. 4c showed a current peak in the positive range of the electric field and P_r was decreased to 13.0 μC/cm^2 owing to thermal depolarization. During the reverse cycle in the negative electric field, two separate peaks were revealed in the switching current and the negative E_C was decreased to -0.24 kV/mm. It is anticipated that the earlier peak was related to the transformation of the ferroelectric-relaxor state, and the later peak resulted from the creation of long-range order along the opposite direction [27, 44, 45]. Even though Fig. 4b also showed the peak splitting of the switching current, there was no decrease out of P_r. The probable reason is relaxor-PT single crystals have both relaxor and normal ferroelectric characteristics with electrically induced long-range ferroelectric order [46–48]. During heat treatment, polar nanoregions (PNRs) of nanosized domains might fluctuate even below T_d because of their smaller domain size compared to larger ferroelectric domains. Therefore, relaxor-PT single crystals with poled state, *i.e.*, electric field-induced ferroelectric state, could show peak splitting of switching current by thermal activation of nano-domains.

In Fig. 5, the TSDC results of [001]-poled rhombohedral PMN-PT single crystals indicated the current and P_r as a function of temperature. Since the spontaneous polarization was reoriented and began to lose its net alignment at a current peak, the thermal depolarization of these materials can be investigated. Figure 5a indicated the two steepest peaks in the vicinity of T_{R-T} and T_C, which were found to be the first T_d and the second T_d, respectively. In the case above T_C, the materials were fully depolarized with no polarization state due to the ferroelectric-to-paraelectric phase transformation. Moreover, the depolarization current peak was not detected during cooling because there was no driving force for the alignment of ferroelectric domains along any specific direction. From the inset in Fig. 5a, it is interesting to note that small currents were detected below the first T_d and gradually increased during heating. On the other hand, remanent polarization (P_r) was obtained by integrating currents with respect to time as shown in Fig. 5b. In calculated P_r (black line), the polarization showed a gradual reduction below the first T_d

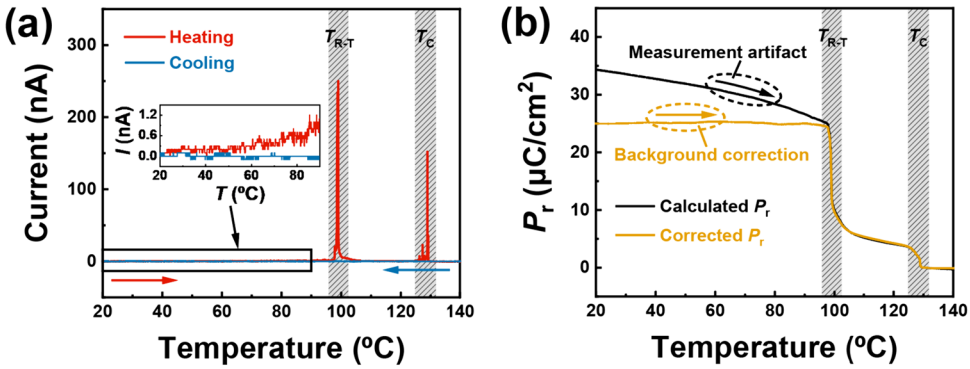

Fig. 5 Thermally stimulated depolarization current (TSDC) results of [001]-poled rhombohedral PMN-PT single crystals for **a** current *vs.* temperature with a magnified temperature range of 20–90 ℃ in the inset and **b** P_r *vs.* temperature obtained from the current data

originating from the small currents, and the depolarization seems to begin even at 20 ˚C. However, the small currents could be a measurement artifact based on the results that there was no degradation of the electrical properties after heat treatment below the first T_d. This phenomenon might be attributed to the reversible contribution of ferroelectric domains or fluctuation of PNRs, resulting in electrical signals while preserving the macroscopic long-range domain configuration, which is consistent with Fig. 4. In corrected P_r (yellow line), the polarization persisted up to the first T_d via a background correction and suddenly reduced in the vicinity of the first T_d. It is expected that the macroscopic long-range order of [001]-poled rhombohedral PMN-PT single crystals would not break in the absence of the phase transformation below T_{R-T}. Therefore, the background correction can be suggested to circumvent such artifact for understanding thermal depolarization and quantitative TSDC measurements of piezoelectric materials.

4 Conclusion

Thermal depolarization of [001]-poled rhombohedral $Pb(Mg_{1/3}Nb_{2/3})O_3$-$PbTiO_3$ (PMN-PT) single crystals was investigated via heat treatment below and above T_d. Rhombohedral-to-tetragonal phase transformation temperature (T_{R-T}) was found to be ~ 98 ℃, which was selected for depolarization temperature (T_d), and Curie temperature (T_C) was determined to be ~ 130 ℃. After heat treatment below T_d, electrical properties remained identically to appear in turn longitudinal piezoelectric coefficient (d_{33} ~ 1480 pC/N), electromechanical coupling factor (k_t ~ 0.54), dielectric permittivity (ε_r ~ 5300), dielectric loss (tan δ ~ 0.0063), and remanent polarization (P_r ~ 23.8 μC/cm^2), whereas the degree of poling was notably degraded after heat treatment above T_d owing to thermal depolarization in the vicinity of T_d. From a thermally stimulated depolarization current (TSDC) measurement, small currents were detected below T_d and gradually increased as approached T_d. However, the small currents could be a measurement artifact since there was no decay of the electrical properties after heat treatment below T_d. It is expected that the macroscopic long-range ferroelectric order would be preserved without the rhombohedral-to-tetragonal phase transformation. Taken together, a background correction is proposed to circumvent the measurement artifact for understanding thermal depolarization and quantitative TSDC analyses of piezoelectric materials.

Acknowledgements This research was supported by the Material Technology Development Program (No. 1415182019) through the Korea Evaluation Institute of Industrial Technology (KEIT). A part of Sun's work was supported by the US National Science Foundation under Grant No. 2309184. Ryu was supported by the US National Science Foundation under Grant No. 2309184.

Data availability The datasets used and/or analyzed during the current study are available from the corresponding author on reasonable request.

Declarations

Conflict of interest The authors declare that there are no conflicts of interest. Wook Jo is an Associate Editor of Journal of the Korean Ceramic Society. Associate Editor status has no bearing on editorial consideration.

References

1. G.H. Haertling, J. Am. Ceram. Soc. **82**(4), 797–818 (1999). https://doi.org/10.1111/j.1151-2916.1999.tb01840.x
2. W. Jo, R. Dittmer, M. Acosta, J. Zang, C. Groh, E. Sapper, K. Wang, J. Rödel, J. Electroceram.Electroceram. **29**(1), 71–93 (2012). https://doi.org/10.1007/s10832-012-9742-3
3. H.-S. Han, T.A. Duong, C.W. Ahn, B.W. Kim, J.-S. Lee, J. Korean Inst. Electr. Electron. Mate. Eng. **36**(5), 433–441 (2023). https://doi.org/10.4313/JKEM.2023.36.5.2
4. H. Jaffe, J. Am. Ceram. Soc. **41**(11), 494–498 (1958). https://doi.org/10.1111/j.1151-2916.1958.tb12903.x
5. S.-H. Go, K.S. Kim, J.S. Kim, C.I. Cheon, J. Korean Ceram. Soc. **60**, 669–678 (2023). https://doi.org/10.1007/s43207-023-00291-8
6. W. Liu, X. Ren, Phys. Rev. Lett. **103**(25), 257602 (2009). https://doi.org/10.1103/PhysRevLett.103.257602

7. J. Rödel, W. Jo, K.T.P. Seifert, E.-M. Anton, T. Granzow, D. Damjanovic, J. Am. Ceram. Soc. **92**(6), 1153–1177 (2009). https://doi.org/10.1111/j.1551-2916.2009.03061.x
8. C. Groh, D.J. Franzbach, W. Jo, K.G. Webber, J. Kling, L.A. Schmitt, H.-J. Kleebe, S.-J. Jeong, J.-S. Lee, J. Rödel, Adv. Funct. Mater.Funct. Mater. **24**(3), 356–362 (2014). https://doi.org/10.1002/adfm.201302102
9. J. Zhang, Z. Pan, F.-F. Guo, W.-C. Liu, H. Ning, Y.B. Chen, M.-H. Lu, B. Yang, J. Chen, S.-T. Zhang, X. Xing, J. Rödel, W. Cao, Y.-F. Chen, Nat. Commun.Commun. **6**(1), 6615 (2015). https://doi.org/10.1038/ncomms7615
10. C.-W. Tao, X.-Y. Geng, J. Zhang, R.-X. Wang, Z.-B. Gu, S.-T. Zhang, J. Eur. Ceram. Soc. **38**(15), 4946–4952 (2018). https://doi.org/10.1016/j.jeurceramsoc.2018.07.006
11. T.T. Zate, J.-W. Sun, N.-R. Ko, B.-K. Koo, H.-L. Yu, M.-S. Kim, W.-J. Choi, S.-J. Jeong, J.-H. Jeon, W. Jo, J. Korean Inst. Electr. Electron. Mater. Eng. **36**(4), 362–368 (2023). https://doi.org/10.4313/JKEM.2023.36.4.6
12. T.T. Zate, N.-R. Ko, H.-L. Yu, W.-J. Choi, J.-W. Sun, J.-H. Jeon, W. Jo, J. Korean Inst. Electr. Electron. Mater. Eng. **36**(3), 214–225 (2023). https://doi.org/10.4313/JKEM.2023.36.3.2
13. A.J. Moulson, J.M. Herbert, *Electroceramics: materials, properties, applications* (John Wiley & Sons, New York, 2003)
14. T.R. Shrout, S.J. Zhang, J. Electroceram.Electroceram. **19**(1), 113–126 (2007). https://doi.org/10.1007/s10832-007-9047-0
15. F. Li, D. Lin, Z. Chen, Z. Cheng, J. Wang, C. Li, Z. Xu, Q. Huang, X. Liao, L.Q. Chen, T.R. Shrout, S. Zhang, Nat. Mater. **17**(4), 349–354 (2018). https://doi.org/10.1038/s41563-018-0034-4
16. S.-E. Park, T.R. Shrout, J. Appl. Phys. **82**(4), 1804–1811 (1997). https://doi.org/10.1063/1.365983
17. S. Zhang, F. Li, J. Appl. Phys. **111**, 031301 (2012). https://doi.org/10.1063/1.3679521
18. E. Sun, W. Cao, Prog. Mater. Sci. **65**, 124–210 (2014). https://doi.org/10.1016/j.pmatsci.2014.03.006
19. D.R. Patil, S.H. Park, G.-T. Hwang, J. Ryu, J. Korean Ceram. Soc. **59**, 322–328 (2022). https://doi.org/10.1007/s43207-021-00172-y
20. A. Von Hippel, Rev. Mod. Phys. **22**(3), 221–237 (1950). https://doi.org/10.1103/RevModPhys.22.221
21. D. Damjanovic, Rep. Prog. Phys. **61**, 1267–1324 (1998). https://doi.org/10.1088/0034-4885/61/9/002
22. M.J. Haun, E. Furman, S.J. Jang, H.A. McKinstry, L.E. Cross, J. Appl. Phys. **62**(8), 3331–3338 (1987). https://doi.org/10.1063/1.339293
23. M.E. Lines, A.M. Glass, *Principles and applications of ferroelectrics and related materials* (Oxford University Press, Oxford, 2001)
24. M. Zhu, H. Hu, N. Lei, Y. Hou, H. Yan, Appl. Phys. Lett. **94**, 182901 (2009). https://doi.org/10.1063/1.3130736
25. Y.A. Genenko, J. Glaum, M.J. Hoffmann, K. Albe, Mater. Sci. Eng. B **192**, 52–82 (2015). https://doi.org/10.1016/j.mseb.2014.10.003
26. B. Kowalski, A. Sehirlioglu, J. Appl. Phys. **121**, 064106 (2017). https://doi.org/10.1063/1.4975785
27. W. Jo, J. Daniels, D. Damjanovic, W. Kleemann, J. Rödel, Appl. Phys. Lett. **102**, 192903 (2013). https://doi.org/10.1063/1.4805360
28. E. Sapper, N. Novak, W. Jo, T. Granzow, J. Rödel, J. Appl. Phys. **115**, 194104 (2014). https://doi.org/10.1063/1.4876746
29. L.M. Riemer, K.V. Lalitha, X. Jiang, N. Liu, C. Dietz, R.W. Stark, P.B. Groszewicz, G. Buntkowsky, J. Chen, S.-T. Zhang, Acta Mater. **136**, 217–280 (2017). https://doi.org/10.1016/j.actamat.2017.07.008
30. H.-P. Kim, C.W. Ahn, Y. Hwang, H.-Y. Lee, W. Jo, J. Korean Ceram. Soc. **54**(2), 86–95 (2017). https://doi.org/10.4191/kcers.2017.54.2.12
31. H. Zhao, Y. Hou, M. Zheng, X. Yu, X. Yan, L. Li, M. Zhu, Mater. Lett. **236**, 633–636 (2019). https://doi.org/10.1016/j.matlet.2018.11.032
32. S. Yang, J. Li, Y. Liu, M. Wang, L. Qiao, X. Gao, Y. Chang, H. Du, Z. Xu, S. Zhang, F. Li, Nat. Commun.Commun. **12**(1), 1414 (2021). https://doi.org/10.1038/s41467-021-21673-8
33. J. Chen, C. Zhou, H. Liu, Q. Li, C. Yuan, J. Xu, J. Wang, J. Zhao, G. Rao, A.C.S. Appl, Mater. Interfaces **15**(8), 10820–10829 (2023). https://doi.org/10.1021/acsami.2c21631
34. H. Song, J.P. Goud, J. Ye, W. Jung, J. Ji, J. Ryu, J. Korean Ceram. Soc. **60**, 747–759 (2023). https://doi.org/10.1007/s43207-023-00305-5
35. C. Bucci, R. Fieschi, Phys. Rev. Lett. **12**(1), 16 (1964). https://doi.org/10.1103/PhysRevLett.12.16
36. E.-M. Anton, W. Jo, D. Damjanovic, J. Rödel, J. Appl. Phys. **10**(1063/1), 3660253 (2011)
37. W. Bai, D. Chen, P. Zheng, B. Shen, J. Zhai, Z. Ji, Dalton Trans. **45**(20), 8573–8586 (2016). https://doi.org/10.1039/C6DT00906A
38. G.-J. Lee, H.-P. Kim, S.-G. Lee, H.-Y. Lee, W. Jo, J. Sensor Sci. Technol. **29**(1), 59–62 (2020). https://doi.org/10.5369/JSST.2019.29.1.59
39. H. Zhang, J. Zhou, J. Shen, Z. Wu, D. He, W. Chen, Appl. Phys. A **127**, 1–9 (2021). https://doi.org/10.1007/s00339-021-04453-5
40. M. Stewart, M. G. Cain and D. Hall, Ferroelectric hysteresis measurement and analysis, (National Physical Laboratory, Teddington 1999).
41. Y. Hosono, K. Harada, T. Kobayashi, K. Itsumi, M. Izumi, Y. Yamashita, N. Ichinose, Jpn. J. Appl. Phys. J Appl Phys. **41**(6), 3808 (2002). https://doi.org/10.1143/JJAP.41.3808
42. J. Xu, H. Deng, Z. Zeng, Z. Zhang, K. Zhao, J. Chen, N. Nakamori, F. Wang, J. Ma, X. Li, H. Luo, Appl. Phys. Lett. **112**(18), 182901 (2018). https://doi.org/10.1063/1.5027591
43. C. Qiu, B. Wang, N. Zhang, S. Zhang, J. Liu, D. Walker, Y. Wang, H. Tian, T.R. Shrout, Z. Xu, L.-Q. Chen, F. Li, Nature **577**(7790), 350–354 (2020). https://doi.org/10.1038/s41586-019-1891-y
44. J.E. Daniels, W. Jo, J. Rödel, V. Honkimäki, J.L. Jones, Acta Mater. **58**(6), 2103–2111 (2010). https://doi.org/10.1016/j.actamat.2009.11.052
45. C.-H. Hong, H. Guo, X. Tan, J.E. Daniels, W. Jo, J. Materiomics **5**(4), 634–640 (2019). https://doi.org/10.1016/j.jmat.2019.06.004
46. F. Li, S. Zhang, T. Yang, Z. Xu, N. Zhang, G. Liu, J. Wang, J. Wang, Z. Cheng, Z.-G. Ye, J. Luo, T.R. Shrout, L.-Q. Chen, Nat. Commun.Commun. **7**(1), 13807 (2016). https://doi.org/10.1038/ncomms13807
47. M.E. Manley, D.L. Abernathy, R. Sahul, D.E. Parshall, J.W. Lynn, A.D. Christianson, P.J. Stonaha, E.D. Specht, J.D. Budai, Sci. Adv. **2**(9), e1501814 (2016). https://doi.org/10.1126/sciadv.1501814
48. G. Liu, L. Kong, Q. Hu, S. Zhang, Appl. Phys. Rev. **10**(1063/5), 0004324 (2020)